Convective Processes in Loose-Fill Attic Insulation—Metering Equipment

Paula Wahlgren

ABSTRACT

A large-scale model of an attic construction has been built in a climatic chamber. The purpose of the attic test model is to investigate heat transfer—in particular, heat transfer by convection—in loose-fill attic insulation. The influence of a number of factors on heat flows can be investigated using the attic test model; for example, insulation thickness, attic ventilation, ceiling construction, roof slopes, and the quality of installation workmanship. The heat flow through the attic ceiling construction is measured with a metering box. The design and calibration of the metering box is described in detail in this paper. During calibration of the metering box, the thermal conductivity of the calibration board was determined within 0.6% of that determined at the Swedish National Testing and Research Institute, SP. Computer simulations carried out to help design the attic test model and to predict the function of the metering box are presented. The location of convection cells in the loose-fill insulation will be determined by investigating the temperature variations on the surface of the insulation by using thermocouples and an infrared camera. The preliminary test program for the attic test model is also presented.

INTRODUCTION

Loose-fill insulation, of mineral wool or cellulose material, is commonly used in attics in Sweden. It has an advantage over insulation boards regarding application, but the loose-fill insulation is more permeable to air, which can cause air movements in the insulation and extra heat loss through the insulation due to convection, especially if the attic is ventilated. The amount of convection not only depends on the material properties of the insulation and the attic ventilation, but also on factors such as insulation thickness, ceiling construction, and workmanship. Consequently, when simulating an attic situation in a laboratory test, the size of the test apparatus is of importance when measuring heat losses. However, in some cases, small-scale measurements can be used to increase the understanding of heat transfer and air movements in the insulation, which is one step to reaching conclusions on how the loose-fill insulation performs in a real attic. Small-scale measurements have been made by Serkitjis (1995), Silberstein et al. (1991), Langlais et al. (1990), and Silberstein et al. (1990). Large-scale measurements made in the U.S. and Canada, by Wilkes et al. (1991), Rose and McCaa (1991), Besant and Miller (1983), and Wilkes and Rucker (1983), show that air movements can occur in the insulation and increase heat loss through the attic ceiling. But the air permeability of the materials used in these countries is higher than that of Swedish material. Swedish large-scale measurements under natural weather conditions (Löfström and Johansson 1992; Anderlind 1992) have not shown any significant heat loss due to air movements. However, in order for the air movements to start, the insulation must be subjected to a large temperature difference (cold winter climate), which was not the case during these measurements. A further review of the literature is found in Fryklund (1997a).

The aim of this project is to understand the heat transfer through loose-fill attic insulation and how it is affected by attic construction, ventilation, and workmanship. The progress of this project is described in Fryklund (1997b). As part of the project, a large-scale attic test model (Figure 1) has been built where the heat flow through the attic ceiling can be measured. A field inventory of attics with loose-fill insulation has been made in order to choose measurement setups. Parallel to the measurements, computer simulations have been made to help predict and analyze the measurements.

Paula Wahlgren (Fryklund) is a Ph.D. student at the Chalmers University of Technology, Göteborg, Sweden.

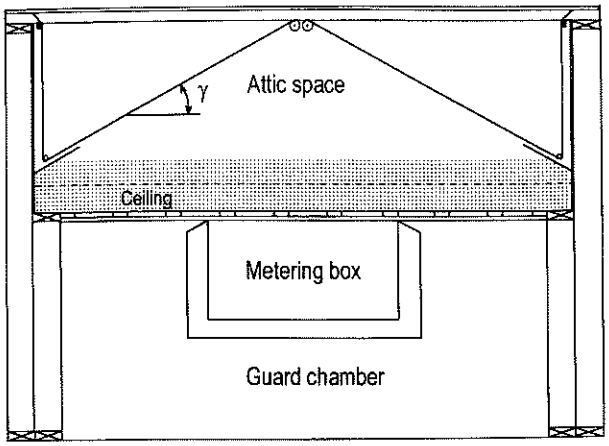

Figure 1 *The plan of the attic test model.*

ATTIC TEST MODEL

An attic test model (6.1 m × 3.3 m × 2.3 m [20 ft × 11 ft × 7.5 ft]) has been built in order to determine the thermal performance of loose-fill insulation when it is installed in an attic ceiling. It is designed so that it will affect the heat flows in the insulation similarly to an actual attic. Using the attic test model, it is possible to investigate how the heat flows are affected by forced convection (attic ventilation), insulation thickness, pitch angle, ceiling construction (including thermal bridges), and inhomogenities in the attic insulation. The attic test model consists of three major parts: the attic space, the ceiling, and the guard chamber. The attic space is constructed of particleboard and, thus, has low thermal resistance. Consequently, the temperature in the attic space will follow that of the climatic chamber (minimum temperature –28°C [–18°F]). Attic space ventilation is simulated by blowing in air along the eaves on one side of the attic. The slope of the roof sides influences the airstreams in the attic and the radiation exchange between the inner attic surfaces. The roof sides in the attic test model are made of reinforced plastic foil, and the pitch angles, γ, of the roof sides are arbitrary ($0 < \gamma < 90°$).

The attic test model ceiling is divided into two equally large parts: one is made of particleboard and one is constructed like an ordinary ceiling (Figure 2). The ordinary ceiling consists of joists (0.045 m × 0.145 m, 1.2 m oc [0.15 ft × 0.48 ft, 3.9 ft oc]), plastic foil, secondary spaced boarding, and gypsum board. The height from the bottom of the ceiling to the roof of the attic space is 1.02 m (3.35 ft), which sets the maximum thickness at which insulation can be applied. Thicknesses of about 0.5 m (1.6 ft) will primarily be used so that the influence of the air movements in the attic space on heat flows through the ceiling can be studied. The heat flows through the insulated ceiling are measured with a metering box. The temperatures in the insulation are measured by thermocouples placed in and on the surface of the insulation. There is one horizontal matrix of thermocouples in each part of the ceiling. A matrix consists of six or seven thermocouples and is designed to detect convection cells of different sizes that may appear at different insulation thicknesses. The investigation into determining the measuring points in the insulation is shown in "Test Procedures." The temperature field on the upper surface of the insulation in the attic test model is also examined with an infrared camera. The guard chamber is the insulated space under the ceiling in the attic test model. It represents the indoor climate of a house and is kept at a temperature of approximately 21°C (70°F).

METERING BOX AND TEMPERATURE MEASUREMENTS

The metering box is used to estimate heat flows through a building component by measuring the amount of heat that is

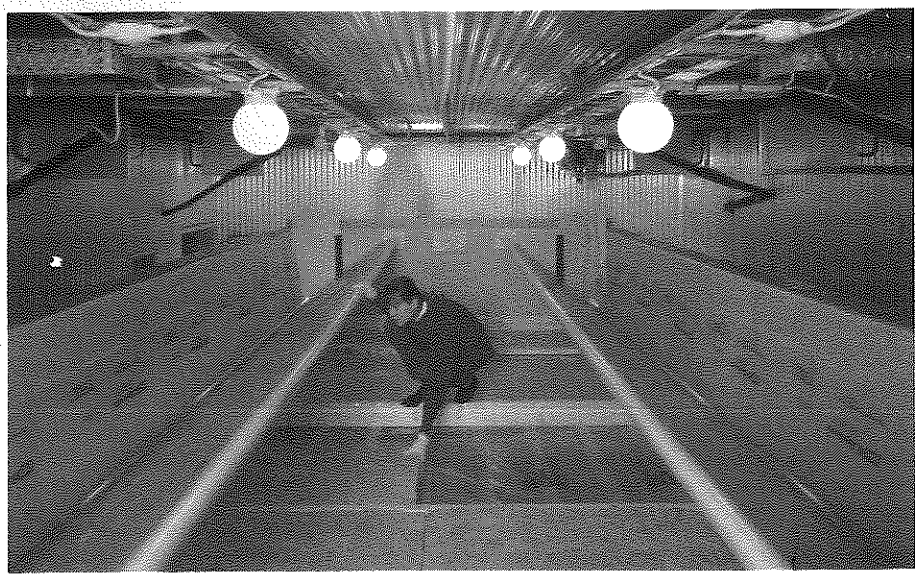

Figure 2 *Top view of the attic space and the ceiling.*

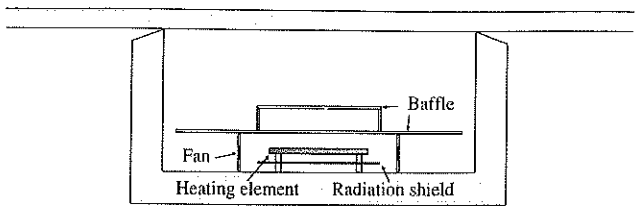

Figure 3 *The metering box.*

produced in the box (by heating elements and by fans) to keep the box at the same temperature as its environment. If the box has exactly the same temperature as the environment, the produced heat passes through the test specimen, in this case the ceiling. The metering box has a metering area of 1.0 m^2 (10.8 ft^2) and is constructed of solid extruded polystyrene with boards of plywood on the inside and outside (Figure 3). A horizontal baffle protects the test specimen from direct radiation from the heating element. The baffle is also used to direct the airflows in the box. The box has four fans and one heating element, and the box surface temperatures are measured with 20 thermocouples. The edge of the metering box in contact with the test specimen is 15 mm (0.59 in.) wide. According to the standard for hot box measurements (ISO 1994), the maximum width is 20 mm (0.79 in.), or 2% of the metering width. The metering box is located on a vertically and horizontally movable platform that can be placed arbitrarily under the ceiling in the attic test model and can be moved at any time.

Heating Element

The heating element is placed at the bottom of the box. Direct current is led through the element, regulated by a proportional-integral-derivative (PID) regulator that controls the temperature via a thermocouple placed directly in front of one of the box fans. The power fed to the element is measured with a digital power meter and integrated over time. The accuracy of the power meter, in the present measurement range, is better than 1%. The maximum required power of the heating element in the box has been estimated to be 18 W (61 Btu/h). With the current setup, the maximum output capacity of the heater is 50 W (170 Btu/h). The influence of temperature fluctuations in the climatic chamber on the temperature in the metering box has been computer simulated (Fryklund 1997b, Hagentoft 1997b), which showed only a small temperature fluctuation in the metering box. This fluctuation is compensated for by the heating element. The temperature difference across the box walls is converted, by a thermopile, into a voltage signal. A regulator uses this signal to control the power output of the heating elements in the guard area so that the temperature difference is minimized. The temperatures under the heating element in the box were measured, and measurements indicated that the heating element only caused a slight increase in surface temperatures in the bottom of the box. Additional temperature measurements also showed that the baffle was effective in blocking radiation between the heating element and the test specimen.

Metering Box Fans and Baffle

The fans are used to get a uniform temperature in the metering box by circulating the air in the box. The air is drawn through a slot in the center of the baffle to the heating element in the bottom of the box. The heating element is surrounded by four fans that blow the air toward the corners of the box and on top of the baffle. Measurements showed that the air velocities and the temperatures were slightly higher (0.15°C - 0.20°C [0.27°F - 0.36°F]) in the corners of the box than at the center of the sides. This was expected since the fans were directed toward the corners. Furthermore, the closer to the heating element, the higher the inner surface temperatures, and the closer to the nose of the box, the lower the inner surface temperatures. All inner surface temperatures are within 1.1°C (2.0°F) when the box is used on a 0.05 m (2 in.) thick board of extruded polystyrene. When the four fans are run simultaneously, the maximum power generated by them is 5.2 W (18 Btu/h). The current through and the voltage over the fans are measured to attain the generated power. The power input to the fans can be regulated. In addition, two, instead of four, fans can be used to further decrease the heat input of the fans when measuring very small heat flows.

Temperature Measurements

The thermocouples used were made of calibrated copper-constantan wires with an absolute accuracy of 0.2°C (0.4°F) and a relative accuracy of 0.1°C (0.2°F), including the error caused by the zero-point calibration in the logger. Two loggers with 31 thermocouples and one thermopile (with 40 thermocouples) were used during the calibration of the metering box. The thermocouple calibration was made in a cryostat at the temperatures 0°C, 10°C, and 20°C (32°F, 50°F, and 68°F). The temperature difference over the metering box surface is measured with 20 thermocouple pairs in series.

METERING BOX CALIBRATION

The metering box is calibrated in a measuring apparatus, the wind box, which is described in detail in Serkitjis (1995) (Figure 4). The wind box has a lower guard chamber and an upper cold chamber, separated by a calibration board (extruded polystyrene, ρ = 36 kg/m^3 [2.2 lb/ft^3], λ = 0.0278 W/m·K [0.193 Btu·in./h·ft^2·°F]).

The guard and the box temperatures ranged from 25°C to 30°C (77°F to 86°F) during the calibration measurements, and the temperature at the cold side was approximately 0°C (32°F). The thermocouples and the power input to the heating elements and the fans have been calibrated separately. The calibration of the box included a number of steps; for example:

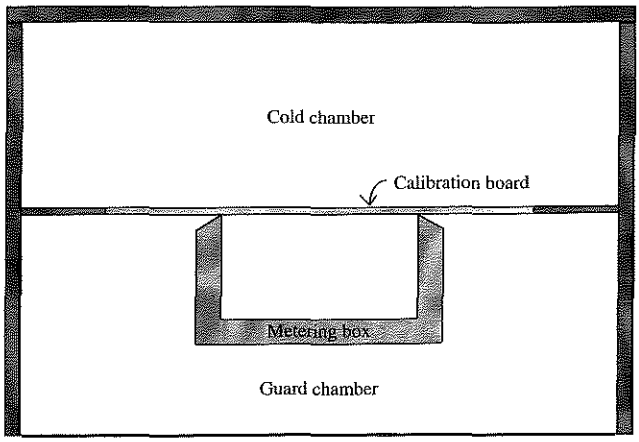

Figure 4 *Calibration setup in the wind box.*

1. Obtaining uniform temperatures in the metering box; previously described.
2. Obtaining uniform temperatures in the guard chamber and on the outer surface of the metering box.
3. Determining the thermal conductance of the box.
4. Determining the thermal conductivity of the calibration board.
5. Determining the heat input to the box; previously described.
6. Determining the proper location of the thermocouples on the box surface.
7. Calibrating the thermocouples and thermopile; previous section.
8. Calculating the thermal conductivity of the calibration board from the measured values of temperature and heat flows, and comparing this with the thermal conductivity measured at the Swedish National Testing and Research Institute, SP.
9. Sensitivity analysis of the metering box.
10. Error analysis of the metering box.

These steps, if not described elsewhere, are briefly described, together with relevant computer simulations, in this section.

Obtaining Uniform Temperatures in the Guard Chamber and on the Outer Surface of the Metering Box. In the guard chamber of the calibration setup in the wind box, two heating elements with radiation shields and two fans were needed to obtain a uniform surface temperature outside the metering box. However, there was a local decrease in temperatures at the nose of the box. This decrease can be explained by a combination of insufficient airflow around the box nose and radiation from the cold calibration board. The amount of radiation was decreased by mounting a layer of aluminum foil on the calibration board outside the metering area (see Figure 5). An estimation of the maximum required airflow was made under the assumption that the temperature difference between

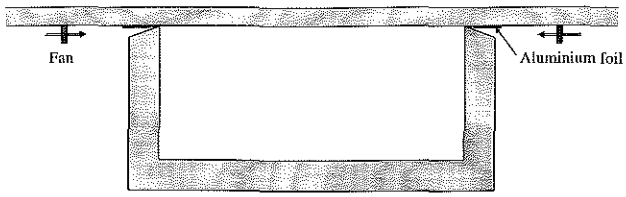

Figure 5 *Measures to adjust the surface temperature of the box nose.*

the inner and outer surfaces of the box nose was 1.0°C (1.8°F). This temperature difference causes a heat flow through the box nose, and this heat flow is compensated for by a warming airflow. The required airflow is estimated to $3 \cdot 10^{-3}$ m^3/min (0.1 ft^3/min). To ensure this airflow, four small fans were installed directly under the calibration board, aimed at the center of each box side nose. With these changes (the fans and the aluminum foil), the outer box surface temperatures were within 1.5°C (2.7°F), previously 1.8°C (3.2°F), and within 0.6°C (1.1°F) when excluding the highest temperature (near one of the guard heating elements). The outer nose surface temperature increased by 0.3°C (0.5°F).

Measurements using the metering box in the attic test model show that neither the fans, the aluminum foil, nor the radiation shields for the guard heating elements are necessary in this setup.

Determining the Thermal Conductance of the Box. The thermal conductance of the metering box, K_{box} (W/K, Btu/h·°F), is the amount of heat loss from the box at a temperature difference of one degree over the box surfaces. The thermal conductance of the metering box was determined to be 1.042 W/K (1.975 Btu/h·°F) using a two-dimensional computer program (Hagentoft 1997a). The conductance is not a critical parameter when calculating the thermal conductivity of a building component. Using the calibration setup as an example, the thermal conductivity of the calibration board increases by 0.01% when the conductance of the box increases by 50%.

Determining the Thermal Conductivity of the Calibration Board. The thermal conductivity of a sample of the calibration board was measured at the Swedish National Testing and Research Institute, SP. The sample included one glued joint and had a thermal conductivity of 0.0278 W/m·K (0.193 Btu·in./h·ft^2·°F) under the same conditions as the calibration setup. The thickness of the sample was 0.0497 m (1.96 in.).

Determining the Proper Location of the Thermocouples on the Box Surface. The original metering box setup had 12 thermocouple pairs to measure the temperature difference across the metering box walls. The thermocouples were equally spaced over the box surface, i.e., two pairs on each box side and four pairs on the bottom of the box. Each thermocouple pair then represented an area of 0.5 m × 0.5 m (1.6 ft × 1.6 ft), i.e., the minimum requirement according to ISO (1994). However, calibration measurements showed that there was a need to improve the accuracy of determining the heat flow

through the metering box and, consequently, that additional thermocouples should be placed on the box. These new thermocouples are located on the upper part of the box, two pairs on each box side, and they account for the heat flow through the box nose. In order to determine the location of these thermocouples, computer simulations were made using the two-dimensional computer program (Hagentoft 1997a). The object of the simulation was to find a new thermocouple location that would result in the correct heat flow being calculated together with existing thermocouples.

The heat flow through the metering box is calculated according to

$$\Phi_{box} = K_{box} \cdot \Delta T_{thermopile} \quad \text{(W, Btu/h)} \qquad (1)$$

where K_{box} (W/K, Btu/h·°F) is the thermal conductance of the box and $\Delta T_{thermopile}$ (K, °F) is the reading from the thermopile to which all the metering box thermocouples are connected.

$$\Delta T_{thermopile} = \frac{1}{20} \cdot \sum_{n=1}^{20} \Delta T_{thermocouples,n} \quad \text{(K, °F)} \qquad (2)$$

From the two-dimensional simulation, the average heat flow per m^2 from the metering box, q_{box} (W/m^2, Btu/h·ft^2), was obtained. Ideally, the same heat flow should be calculated when using readings from the thermocouples.

$$q_{box} = \frac{K_{box}}{A_{box,i}} \cdot \sum_{n=1}^{20} \Delta T_{thermocouples,n} = \sum_{n=1}^{20} q_{thermocouple,n} \quad \text{(W/m}^2\text{, Btu/h·ft}^2\text{)} \qquad (3)$$

Twelve thermocouple pairs are already fixed, so the location of the eight thermocouple pairs that will measure the heat flow through the upper part of the box, near the nose, is to be determined so that Equation 3 will be fulfilled (see Figure 6).

The heat flow that would balance the originally measured heat flows was found at a distance of 0.058 m (2.3 in.) from the nose, where currently eight thermocouple pairs, two pairs on each box side, are placed.

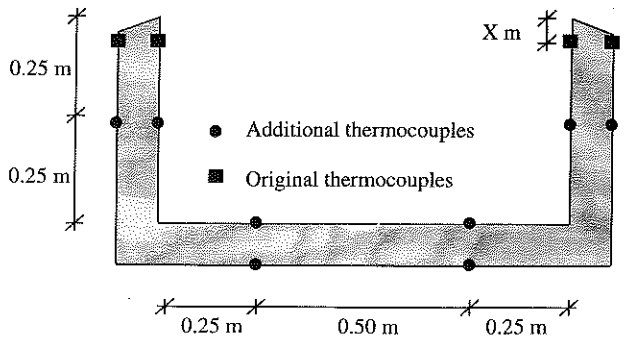

Figure 6 *Determination of the location of eight additional thermocouple pairs.*

Calibration Result

The careful placement of the thermocouples, in combination with efforts to attain an isotherm outer and inner box surface as previously described, resulted in a thermal conductivity of the calibration board within 0.6% of that measured at SP.

The thermal conductivity of the board was calculated according to the following procedure:

$$\Phi_{box} = K_{box} \cdot \Delta T_{box} \quad \text{(W, Btu/h)} \qquad (4)$$

$$\Phi_{cal} = \Phi_{input} - \Phi_{box} \quad \text{(W, Btu/h)} \qquad (5)$$

$$\lambda_{cal} = \frac{\Phi_{cal} \cdot d_{cal}}{\Delta T_{cal}} \cdot \frac{1}{A} \quad \text{(W/m·K, Btu·in./h·ft}^2\text{·°F)} \qquad (6)$$

where

ΔT_{cal} = temperature difference over the calibration board within the metering area; mean value of two thermocouples on the cold side and five on the warm side (K, °F).

d_{cal} = thickness of the calibration board according to SP (m, ft).

A = metering area (m², ft²).

ΔT_{box} = temperature difference over the box walls, measured with 20 thermocouple pairs (K, °F).

K_{box} = thermal conductance of the metering box (W/K, Btu/h·°F).

Φ_{input} = heat input from the heating element and the fans in the box (W, Btu/h).

ΔT_{cal} = 26.06 K (47.0°F), d_{cal} = 0.0497 m (0.163 ft), A = 1.006 m^2 (10.83 ft^2), ΔT_{box} = –0.028 K (–0.050°F), K_{box} = 1.042 W/K (1.975 Btu/h·°F), Φ_{input} = 14.71 W (50.2 Btu/h).

This results in a thermal conductivity of the calibration board of 0.02794 W/m·K (0.1938 Btu·in./h·ft^2·°F), and compared with the thermal conductivity measured at SP, 0.0278 W/m·K (0.1928 Btu·in./h·ft^2·°F), the error is less than 0.6%.

Sensitivity Analysis

This section includes simulations, using the two-dimensional computer program, that have been made to determine how the metering box affects and responds to its environment. When possible, the simulations are compared with measurements. Further simulations are described in Fryklund (1997b, 1995).

Heat Losses Through the Ceiling Sides. The construction of the ceiling in the attic test model has been simulated to investigate if the attic ceiling is wide enough to allow heat flow measurements that are not disturbed by edge effects. The edge effects, in this case, mean heat that flows from the metering area along the ceiling construction to the climatic chamber.

The guard chamber temperature is 20°C (68°F), R_{si} = 0.15 m^2K/W (0.85 $ft^2 \cdot h \cdot °F/Btu$), and the attic space temperature is −28°C (−18.4°F), R_{se} = 0.20 m^2K/W (1.1 $ft^2 \cdot h \cdot °F/Btu$), which obtains the worse case. The ceiling is 3.01 m (9.88 ft) wide, and the simulation shows that the center of the ceiling is undisturbed by the edge losses. When the insulation is 0.5 m (1.6 ft) thick, a 1% (0.28°C [0.50°F]) decrease in the temperature of the lower surface is found at a distance of 0.22 m (0.72 ft) from the wall. Next to the wall, the corresponding percentage is 11% (3.1°C [5.6°F]).

Surface Temperatures Outside the Box. Four simulations have been made to investigate how the heat flows measured by the metering box are affected by increased surface temperatures on the metering box, the nose, the lower surface of the ceiling outside the box, or combinations of these. The simulation setups are shown in Figures 7a, 7b, and 7c. The thick dark-gray lines represent surfaces with a temperature of 1°C (34°F) and the thin black lines a temperature of 0°C (32°F).

The simulations are for the calibration configuration, i.e., the metering box applied to a 0.05 m (2 in.) thick extruded polystyrene board. Setup B has also been simulated with a particleboard under the polystyrene board to simulate the situation when the box is used in the attic test model. Since a particleboard has a lower thermal resistance than a polystyrene board, the influence of the increased surface temperature under the ceiling will be greater. However, the total thermal resistance of the boards (or board) is maintained in all simulations. The results are presented as the amount of heat that flows into the metering box. A heat flow into the box would result in less heat being produced by the heating element and the calculation of a thermal resistance of the ceiling that is too low. Setup A results in a heat flow of 1.04 W (3.55 Btu/h) at a temperature difference of 1°C (1.8°F). Since the produced heat flow in the box is in the range of 0.5 W to 18 W (1.7 Btu/h to 61 Btu/h), this gives a large error and must be avoided. Setup B shows that the error in Setup A was not caused by the nonuniform ceiling temperature since that only causes an increase of 0.04 W (0.1 Btu/h). When an increase in outer nose temperature is added to Setup B, the heat flow increases to 0.30 W (1.0 Btu/h), which is not acceptable. Setup B with a particleboard results in a heat flow of 0.24 W (0.82 Btu/h), which is substantially higher than without the particleboard. The conclusion of this investigation is that it is essential that the heating elements and fans are regulated and placed so that a uniform temperature is reached on all the surfaces in the guard. This has also been investigated in the calibration setup in the wind box and has previously been described.

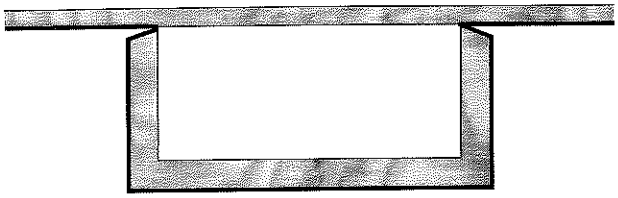

Figure 7a *Setup A, warmer outer surfaces.*

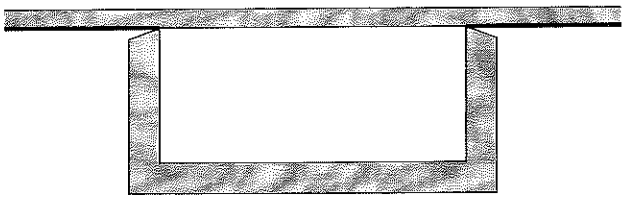

Figure 7b *Setup B, warmer ceiling surface.*

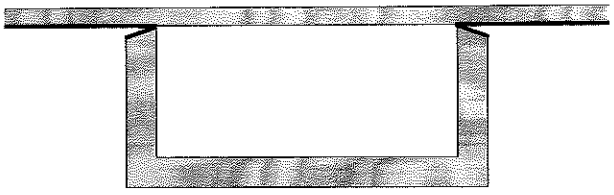

Figure 7c *Setup C, warmer ceiling and outer nose surfaces.*

Surface Temperatures Inside the Box. In order to determine the best possible uniformity of the inner surface temperatures of the box and the lower surface of the calibration board in the metering area, the box was simulated with surface resistances in the calibration setup. All surface resistances, that is inner and outer box surfaces and lower and upper calibration board surfaces, were 0.1 m^2K/W (0.57 $ft^2 \cdot h \cdot °F/Btu$). The air temperatures in the box and the guard were 28.8°C (83.8°F), and the air temperature on top of the calibration board was 0°C (32°F). The simulations showed that the temperature of the upper part of the inner box wall surface was lowered by 0.15°C (0.27°F), i.e., 0.52% of the temperature difference across the calibration board. A corresponding measured temperature difference in the calibration setup was 0.39°C (0.70°F). This larger decrease is probably due to a greater surface resistance at the top of the wall caused by slightly lower air velocity since the fans are placed at the bottom of the box. At a distance of 0.08 m (0.26 ft) from the top of the wall, in the simulation, the decrease in temperature was not detectable. The lower surface of the calibration board was 27.21°C (80.98°F) next to the box wall and 27.36°C (81.25°F) at 0.8 m (2.6 ft) of the 1 m (3.3 ft) wide metering area. Corresponding measured temperatures in the calibration setup were less uniform. There was a difference of 1.0°C (1.8°F) between the calibration board surface temperatures within the metering area, where an increase in temperature was found next to the metering box nose, in a corner. The other surface temperatures were within 0.6°C (1.1°F). According to the standard for hot box measurements (ISO 1994), the surface temperatures in the measuring area may differ by 2% of the temperature difference over the test specimen, in this case 0.6°C (1.1°F) or 2 K/m (1.1°F/ft). Apart from the simulated temperatures, solely caused by conduction, the surface temperatures are also affected by airflows in

the box and by heat flows to or from the metering area.[1] The increased surface temperature in the box corner is probably caused by a flow of warm air. The fans in the metering box are directed toward the corners of the box, and as a result, the largest upward flow of heated air around the baffle is in the corners. The conclusion to be drawn from this investigation is that we must accept that the measured surface temperatures in the box vary slightly due to conduction in the material and to airflows in the box. However, the calibration board has a lower thermal resistance than the ceiling with insulation in the attic test model; subsequently, the discussed surface temperatures will, in most cases, be more uniform in the attic test model than in the calibration setup.

Error Analysis

An error analysis of the metering box shows that the maximum error in determining the thermal resistance of a building component is 3%. The analysis is made under the assumption that the heat flow through the metering box walls is zero. Calculations with measured values from the calculation setup show that this heat flow ranges from 3 mW to 32 mW (0.01 Btu/h to 0.1 Btu/h) during a measurement period. An investigation of the influence of imbalanced wall temperatures on heat flows is found in the previous section. Other assumptions made for the error analysis are that stationary conditions are obtained and that surface temperatures are uniform (the effect of nonuniformities is discussed in the previous section). The error analysis is based on the following formula that states that the maximum error is the sum of the relative error of each variable.

$$\Delta F = \left| \sum_{k=1}^{n} \frac{\partial F}{\partial x} \Delta x_k \right| \qquad (7)$$

The formula for determining the thermal resistance of a building component is

$$R_{comp} = \frac{A \cdot \Delta T_{comp}}{\Phi_{comp}} \ (\mathrm{m^2K/W,\ ft^2 \cdot h \cdot {}^\circ F/Btu}) \qquad (8)$$

where

Φ_{comp} = heat flow rate through the building component (W, Btu/h),

A = area over which the heat flow is measured (m^2, ft^2),

ΔT_{comp} = surface to surface temperature difference over the building component (°C, °F).

Using the attic test model and the metering box, this formula becomes

$$R_{comp} = \frac{l^2 \cdot \Delta T_{comp}}{\Phi_{input}} \ (\mathrm{m^2K/W,\ ft^2 \cdot h \cdot {}^\circ F/Btu}) \qquad (9)$$

where l^2 is the metering area of the box.

The maximum relative error is

$$\frac{\delta R_{comp,max}}{R_{comp}} = \left| \frac{2}{l} \cdot \delta l \right| + \left| \frac{1}{\Delta T_{comp}} \cdot \delta(\Delta T_{comp}) \right| + \left| \frac{1}{\Phi_{input}} \cdot \delta \Phi_{input} \right| \quad (\%) \qquad (10)$$

The length of the box side is measured with a steel ruler with an accuracy of $5 \cdot 10^{-4}$ m ($2 \cdot 10^{-3}$ ft). The temperature difference over the building component, ΔT_{comp}, is measured with an accuracy of 0.1°C (0.2°F). According to the manufacturer, the heat input is measured within 1%, i.e., $\delta\Phi_{input}/\Phi_{input}$ is 0.01. The maximum relative error will be the greatest when measuring at low temperature differences over the component, maximum for $\delta(\Delta T_{comp})/\Delta T_{comp}$. The minimum temperature difference to be used in the attic test model is approximately 10°C (18°F). Under these assumptions, the maximum relative error $\delta R_{comp,max}/R_{comp}$ becomes 3%.

TEST PROCEDURES

The measurements to be carried out in the attic test model will include measurements of different insulation thicknesses, varying ventilation, and different roof slopes. Furthermore, the construction of the ceiling and the quality of installation workmanship will be investigated. The ceiling consists of two parts: one part is constructed like an ordinary ceiling, and one part has only particle board and plastic foil under the insulation. The homogeneous part is used to investigate the performance of the insulation without the influence of the normal ceiling construction.

Preliminary Test Program

Initial calibration measurements have been made using low-permeable mineral boards to determine the appropriate location of heating elements and fans in the guard and the thermocouple location on the lower and upper surface of the ceiling. The thermocouple location on the upper surface of the insulation with respect to the detection of convection cells is described in the section "Measurement Analysis and Strategy." After the calibration, measurements will probably first be carried out with a common loose-fill mineral wool to study the effects of convection (if any) in a normal attic insulation. To draw conclusions about a wider range of insulation materials, a more permeable loose-fill mineral wool will later be applied. Each loose-fill insulation will be investigated at different insulation thicknesses, using three pitch angles and a varying ventilation rate. The investigations into workmanship, installations, and deficiencies include several configurations and will be performed last.

Possible configurations follow:

- A cavity at the insulation surface, caused by men or mice.
- A cavity at the insulation surface next to a joist, caused by settling of the material.
- A cavity at the insulation surface next to the eaves. This

1. Additional simulations showed that a temperature difference of 0.5°C (0.9°F) on the lower surface of the calibration board, over the metering box edge, induced a heat flow of 0.04 W (0.14 Btu/h) to, or from, the metering area, or vice versa.

kind of cavity is due to a very high rate of attic ventilation or poor workmanship when installing the baffles that prevent the ventilation air from blowing directly through the insulation.

- A cavity inside the insulation, caused by mice.
- An installation (pipe) in the insulation.
- An installation in combination with settling of the insulation that would create an air cavity under the insulation.

In order to choose the most interesting configurations, the results of a field attic inventory will be used and computer simulations will be made. Some of the configurations will also be tested in a small-scale apparatus, the wind box.

Measurement Analysis and Strategy

Since the purpose of the measurements is to determine the total heat transfer, and in particular to study the convective heat transfer through an attic insulation, the convective heat transfer needs to be described. There are several dimensionless parameters for describing convective heat transfer in porous materials, sometimes in combination with conductive and radiative heat transfer. The Nusselt number, Nu, and the modified Rayleigh number, Ra_m, are frequently used. The Nusselt number describes the total amount of heat transferred in a convective situation compared to the amount of heat transferred in a nonconvective state. The Nusselt number is often given as a function of the modified Rayleigh number, Ra_m. The modified Rayleigh number increases with increasing tendency to develop convective air movements in a material. See Nield and Bejan (1992) for a more extensive description.

The Nusselt number is defined by

$$Nu = \frac{q^{slab}_{with\ convection}}{q^{slab}_{without\ convection}} \quad (-) \qquad (11)$$

where q^{slab} should be considered as the average heat flow over the whole slab. When there is no convection, the Nusselt number is equal to one.

The modified Rayleigh number, Ra_m, is defined as

$$Ra_m = \frac{\rho \cdot c_p \cdot g \cdot \beta \cdot \Delta T \cdot k \cdot d}{\nu \cdot \lambda} \quad (-) \qquad (12)$$

As pertains to air, c_p (J/kg·K, Btu/lb·°F) is the specific heat capacity of the air, ρ (kg/m^3, lb/ft^3) is the density, $\beta = 1/T_{mean}$ (1/K, 1/°F) is the heat expansion coefficient, and ν (m^2/s, ft^2/s) is the kinematic viscosity. The air permeability of the porous material is denoted as k (m^2, ft^2), and λ (W/m·K, Btu·in./h·ft^2·°F) is the thermal conductivity of the insulation without convection. ΔT (°C, °F) is the temperature difference over the insulation and d (m, ft) is the insulation thickness. The modified Rayleigh number is used to estimate the magnitude of the convective forces, which depends on all of the parameters mentioned above, the boundary conditions, and the aspect ratio of the width and the thickness of the material. The boundary conditions at the top and the bottom are related to temperature (isothermal or nonisothermal) and to permeability (permeable or impermeable).

In addition to studying the heat flows, convection can also be investigated by studying the temperature profiles in and on the surface of the insulation. When the convective air movements in the insulation start, convection cells are created. The shape of the convection cells depends on factors such as the geometry of the insulation layer, the boundary conditions, and the modified Rayleigh number. In the part of the test model ceiling that contains joists, the cells will probably be cylindrical since the joists are thermal bridges and will cause an upward heat flow in their vicinity. In the homogeneous part of the ceiling, however, the cells can be circular or cylindrical or have more complex shapes. To detect these cells, a matrix of thermocouples can be used and placed either in the loose-fill insulation or on top of the insulation. There are several advantages to placing the thermocouples on the insulation surface. First, the thermocouples can also be used when determining the thermal resistance of the ceiling. Second, the thermocouples can easily be moved. Third, since the thermocouples are visible, it is easier to determine the location, especially height, of the thermocouples and to check that they have not been dislocated. There is one disadvantage to placing the thermocouples on top of the insulation, which is a possible lack in temperature variation at the surface if the attic ventilation rate is high (low thermal surface resistance). Computer simulations, using a three-dimensional program (Hagentoft and Serkitjis 1995), have been made on the homogeneous part of the ceiling. Figure 8, from the simulations, shows an example of the temperature distribution on the upper surface of the insulation from above.

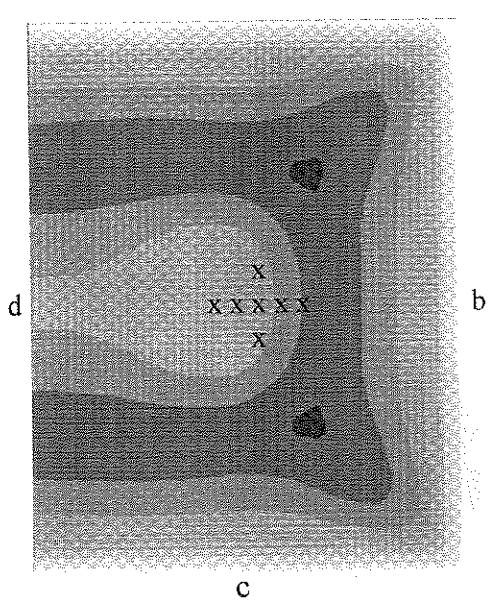

Figure 8 *The upper surface of an attic insulation in contact with three cold walls (a, b, c). Surface temperatures range from −30°C to −25°C (−22°F to −13°F).*

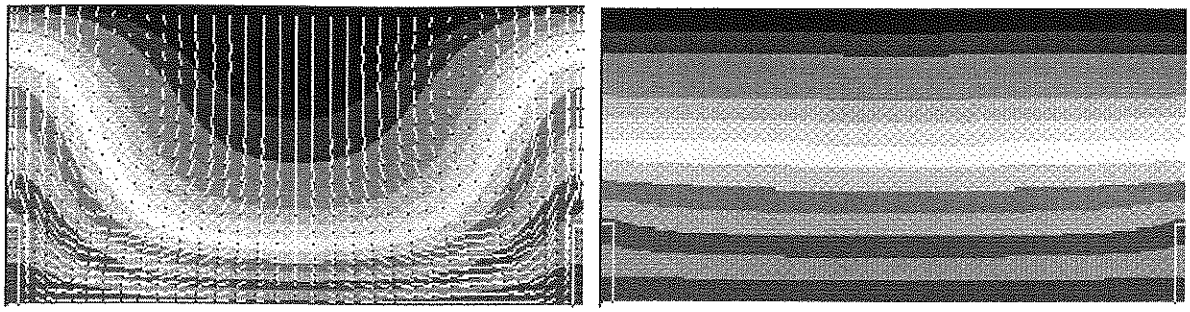

Figure 9 *Isotherms and airflows in a cross section of the ceiling. Convection is included in the left simulation showing two cylindrical cells.*

Walls a, b, and c have the same temperature as the attic space, and wall d is adiabatic (in contact with the normal ceiling part). In order to detect if there are convection cells in the insulation in the attic test model, a two-dimensional matrix is placed on top of the ceiling. The matrix has seven thermocouples with a spacing of 0.2 m (0.7 ft) (Figure 8).

In the normal part of the ceiling (with joists), the matrix has six thermocouples. This ceiling part has been simulated with the two-dimensional computer program (Hagentoft 1995). The simulations have been made using different temperatures on the upper surface, with and without natural convection included in the simulation, and using an upper thermal surface resistance of 0.2 m^2K/W (1.1 $ft^2 \cdot h \cdot °F/Btu$), as suggested by Serkitjis (1995) for natural convection. The purpose is to see what temperature disturbance natural convection will cause on the upper surface, to ensure that the magnitude of the disturbance can be detected using thermocouples. Figure 9 represents one of the simulations; insulation thickness 0.545 m (1.79 ft), with and without convection, showing the isotherms and airflow directions in a cross section of the ceiling. One bay is displayed.

The temperature difference along the upper surface is 1.8°C (3.2°F), in this case 8% of the total temperature difference across the insulation when convection is included in the simulation. This difference is detectable with the thermocouple matrix previously described. When there is no convection in the simulation, the upper surface has no detectable temperature gradient along the surface. Thermography will occasionally be used to investigate the surface temperatures of the attic insulation during measurements.

A vertical temperature profile through the insulation was also investigated. The location of the profile is next to a joist. When comparing the temperature profile of the simulations with convection and without convection, it is evident that the airflows disturb the temperature profiles in the insulation. The temperature at the top of the joist differs by 1.5°C (2.7°F) when comparing the simulations with and without convection. These findings resulted in the location of a thermocouple at the top of a joist in the attic test model. There are more significant temperature differences in the insulation, for example, 3.5°C (6.3°F) at 1.5 cm (0.59 in.) from the top surface of the insulation. However, placing a thermocouple on a joist ensures that the thermocouple will not be displaced. The air temperatures in the metering box and in the attic space will also be measured so that a thermal transmittance, U, can be calculated for the ceiling. The location of the thermocouples measuring the air temperature in the attic is yet to be determined. The location depends on the result of measurements currently being made of heat flow losses through the insulation as a function of wind speed over the insulation within another project at the department.

CONCLUSIONS

A large-scale attic test model that is constructed to study heat transfer through an attic ceiling insulated with loose-fill insulation is described in this paper. The error analysis of the heat flow metering box showed that the maximum relative error when determining the thermal resistance of a ceiling with insulation is 3%. During calibration measurements, the thermal conductivity of the calibration board (extruded polystyrene) was determined within 0.6% of that determined at the Swedish National Testing and Research Institute, SP. An analysis of how the metering box affects and responds to its environment is shown in the section "Sensitivity Analysis." The preliminary test program, including measurements with different roof slopes, varying ventilation, different insulation thickness, and a number of deficiencies in the loose-fill insulation, is presented. The location of the thermocouples in and on the surface of the loose-fill to indicate convection is also discussed.

ACKNOWLEDGMENTS

This project is financially supported by the Swedish Council for Building Research (BFR) and Swedisol. Their grants are greatly appreciated. The research is being carried out under the inspiring guidance of Professor Carl-Eric Hagentoft and Claes Bankvall.

NOMENCLATURE

A = area (m^2, ft^2)

c_p = specific heat capacity at constant pressure (J/kg·K, Btu/lb·°F)

d = thickness (m, ft)

g = gravitational acceleration (m/s^2, ft/s^2)
k = air permeability (m^2, ft^2)
l = length (m, ft)
Nu = the Nusselt number (–)
q = density of heat flow rate (W/m^2, $Btu/ft^2 \cdot h$)
R = thermal resistance (m^2K/W, $ft^2 \cdot h \cdot °F/Btu$)
Ra = the Rayleigh number (–)
T = temperature (°C, K, °F)
U = thermal transmittance (W/m^2K, $Btu/h \cdot ft^2 \cdot °F$)
β = heat expansion coefficient (1/K, 1/°F)
γ = pitch angle (°)
λ = thermal conductivity ($W/m \cdot K$, $Btu \cdot in./h \cdot ft^2 \cdot °F$)
ρ = density (kg/m^3, lb/ft^3)
ν = kinematic viscosity (m^2/s, ft^2/s)
Φ = heat flow rate (W, Btu/h)
K_{box} = thermal conductance of the metering box (W/K, Btu/h·°F)

Subscripts and Superscripts

e = exterior
i = interior
m = porous medium
s = surface

Most physical quantities and definitions are in accordance with ISO (1987a, 1987b).

REFERENCES

Anderlind, G. 1992. Multiple regression analysis of in situ thermal measurements—Study of an attic insulated with 800 mm loose fill insulation. *Journal of Thermal Insulation and Building Envelopes*, Vol. 16, July.

Besant, W., and E. Miller. 1983. Thermal resistance of loose-fill fiberglass insulation in spaces heated from below. *ASHRAE/DOE Proceedings, Conference on the Thermal Performance of the Exterior Envelopes of Buildings II*, ASHRAE SP 38, pp.720-733.

Fryklund, P. 1995. Computer investigations on heat transfer in loose-fill attic insulation. Report 870 R-95:5, Department of Building Physics, Chalmers University of Technology, Sweden.

Fryklund, P. 1997a. A review of the literature on convective processes in loose-fill attic insulation. Report 881 R-97:3, Department of Building Physics, Chalmers University of Technology, Sweden.

Fryklund, P. 1997b. Convective processes in loose-fill attic insulation—Metering equipment. Licentiate thesis, Report 894 P-97:3, Department of Building Physics, Chalmers University of Technology, Sweden.

Hagentoft, C-E. 1995. CHConP—Convection heat conduction program. Personal Communication.

Hagentoft, C-E. 1997a. HConP—Heat conduction program, Building physics fundamentals. Report 885 R-97:1, Department of Building Physics, Chalmers University of Technology, Sweden.

Hagentoft, C-E. 1997b. P-Krets, Building physics fundamentals. Report 885 R-97:1, Department of Building Physics, Chalmers University of Technology, Sweden

Hagentoft C-E, and M. Serkitjis. 1995. Simplified models for natural and forced convection in porous media, International symposium on moisture problems in building walls. Porto, Portugal, pp. 339-350, or Report R-95:8, Department of Building Physics, Chalmers University of Technology, Sweden.

ISO. 1994. *ISO 8990, Thermal insulation—Determination of steady-state thermal transmission properties—Calibrated and guarded hot box.* International Standard Organization.

ISO. 1987a. *ISO 9346, Thermal insulation—Mass transfer—Physical quantities and units.* International Standard Organization.

ISO. 1987b. *ISO 7345, Thermal insulation—Physical quantities and definitions.* International Standard Organization.

Langlais, C., E. Arquis, and D.J. McCaa. 1990. A theoretical and experimental study of convective effects in loose-fill thermal insulation, Insulation materials: Testing and applications. *ASTM STP 1030*, pp. 290-318. Philadelphia.

Löfström, R., and C. Johansson. 1992. Lösfyllnadsisolering på bjälklag—Bestämning av värmemotstånd, Swedish National Testing and Research Institute, SP Report 1992:62, ISBN 91-7848-381-6, ISSN 0284-5172 [Available in Swedish only].

Nield, D.A., and A. Bejan. 1992. *Convection in porous media.* Springer-Verlag New York Inc., 408 p.

Rose, W.B., and D.J. McCaa. 1991. The effect of natural convective airflows in residential attics on ceiling insulation materials. *Insulation materials: Testing and applications*, Vol. 2, pp. 263-291. Philadelphia.

Serkitjis, M. 1995. Natural convection heat transfer in a horizontal thermal insulation layer underlying an air layer. Thesis, Department of Building Physics, Chalmers University of Technology, Sweden.

Silberstein, A., E. Arquis, and D.J. McCaa. 1991. Forced convection effects in fibrous thermal insulation. *Insulation materials: Testing and applications*, Vol. 2, pp. 292-309. Philadelphia.

Silberstein, A., C. Langlais, and E. Arquis. 1990. Natural convection in light fibrous insulating materials with permeable interfaces: Onset criteria and its effect on the thermal performance of the product. *Journal of Thermal Insulation*, Vol. 14, pp. 22-42.

Wilkes, K.E., and J.L. Rucker. 1983. Thermal performance of residential attic insulation. *Energy and Buildings*, Vol. 5, pp. 263-277.

Wilkes, K.E, R.L. Wendt, A. Delmas, and P.W. Childs. 1991. Thermal performance of one loose-fill fiberglas attic insulation. *Insulation materials: Testing and application*, Vol. 2, pp. 275-291. Philadelphia.